REPORT 1167

METHOD FOR CALCULATING THE ROLLING AND YAWING MOMENTS DUE TO ROLLING FOR UNSWEPT WINGS WITH OR WITHOUT FLAPS OR AILERONS BY USE OF NONLINEAR SECTION LIFT DATA [1]

By ALBERT P. MARTINA

SUMMARY

The methods of NACA Reports 865 and 1090 have been applied to the calculation of the rolling-moment and yawing-moment coefficients due to rolling for unswept wings with or without flaps or ailerons. The methods are based on lifting-line theory and allow the use of nonlinear section lift data. The method presented herein permits calculations to be made somewhat beyond maximum lift for wings having no twist or continuous twist and employing airfoil sections which do not display large discontinuities in the lift curves. Calculations can be made up to maximum lift for wings with discontinuous twist such as that produced by partial-span flaps or ailerons, or both. Two calculated examples are presented in simplified computing forms in order to illustrate the procedures involved.

INTRODUCTION

The calculation of the rolling-moment and yawing-moment coefficients due to rolling has received extensive treatment in the linear lift range; several of the better-known sources are references 1 to 3. Methods for making the calculations in the nonlinear lift range, however, are comparatively few (for example, refs. 4 to 6) and are based on the overall lift and drag of a wing.

Methods for calculating wing characteristics in the nonlinear lift range by using lifting-line theory and nonlinear section data (refs. 7 and 8) have given estimates which agree closely with results of wind-tunnel tests of nonrolling wings, as seen in references 8 and 9. It was believed, therefore, that these methods could be utilized in the calculation of the rolling derivatives and that such calculations might be more accurate than those made by existing methods.

Although the application of the lifting-line method to a rolling wing in the nonlinear range is implicitly contained in reference 7 and partially illustrated in reference 8, it is the purpose of the present report to outline the procedure of calculation by means of several illustrative examples. In addition, some new considerations regarding the application of these methods to the calculation of the rolling characteristics are presented and discussed. Because of the supplementary nature of this report, the reader should be reasonably familiar with references 7 and 8.

SYMBOLS

The term "section" as used herein denotes the section characteristics in three-dimensional flow.

A	aspect ratio
C_D	wing drag coefficient
C_l	wing rolling-moment coefficient
C_{l_p}	coefficient of wing damping in roll, $\partial C_l \Big/ \partial\left(\frac{pb}{2V}\right)$
C_L	wing lift coefficient
C_n	wing yawing-moment coefficient
C_{n_p}	coefficient of wing yawing moment due to rolling, $\partial C_n \Big/ \partial\left(\frac{pb}{2V}\right)$
E	effective edge-velocity factor for symmetrical part of lift distribution, $\sqrt{1+\frac{4}{A^2}}$
E'	effective edge-velocity factor for antisymmetrical part of lift distribution, $\sqrt{1+\frac{16}{A^2}}$
F	factor used in altering two-dimensional lift curves
K, K_t	coefficients used in obtaining succeeding approximations of lift distribution
R	Reynolds number
V	velocity
a_0	two-dimensional linear lift-curve slope
b	wing span
c	local chord of wing
c_r	root chord
$\bar{c}$	mean geometric chord, b/A
c_{d_0}	section profile-drag coefficient
$(c_{d_0})_0$	two-dimensional profile-drag coefficient
c_l	section lift coefficient
$c_{l_{al}}$	additional section lift coefficient for $C_L=1.0$
c_{l_0}	two-dimensional lift coefficient
$c_{l_{max}}$	maximum section lift coefficient
$(c_{l_{max}})_0$	maximum two-dimensional lift coefficient
$c_{l(\delta)}$	section lift coefficient for a particular flap deflection
p	angular rolling velocity, radians/sec

[1] Supersedes NACA TN 2937, "Method for Calculating the Rolling and Yawing Moments Due to Rolling for Unswept Wings With or Without Flaps or Ailerons by Use of Nonlinear Section Lift Data" by Albert P. Martina, 1953.

r number of intervals between points of calculation along span
t maximum thickness of wing section
y spanwise coordinate
α angle of attack, deg
α_c correction for induced angle of attack, deg
α_e effective angle of attack, deg
α_i induced angle of attack, deg
α_{i_0} angle of attack for zero lift, deg
α_0 angle of attack for two-dimensional lift curves, deg
α_s angle of attack of root section, deg
α_u uncorrected induced angle of attack, deg
β_{mk} induced angle-of-attack multiplier for asymmetrical distribution
δ magnitude of discontinuity in absolute and induced angles of attack, deg
ϵ geometric angle of twist, negative if washout, deg
$\bar{\epsilon}$ approximate average angle of twist,

$$\frac{A}{2}\int_{-1}^{1}\epsilon\left[\frac{\frac{c}{\bar{c}}+1.273\sqrt{1-\left(\frac{2y}{b}\right)^2}}{2A+3.6}\right]d\frac{2y}{b},\ \text{deg}$$

ϵ_p angle of twist due to rolling motion, deg
ϵ_t angle of twist at wing tip, deg
λ taper ratio (ratio of tip chord to root chord)
η ratio of actual two-dimensional lift-curve slope to theoretical value of $\pi^2/90$
η_m area multiplier for asymmetrical distributions
ν_m interpolation multiplier
σ_m moment multiplier for asymmetrical distributions

Superscript:

$*$ denotes value at end of flap or aileron

CALCULATION PROCEDURE

Inasmuch as complete theoretical developments of the method used herein are given in references 7 and 8, only the items pertinent to the purpose of the present report will be given. The method is based on lifting-line theory and uses the effective edge-velocity factors E and E' to correct for the effects of aspect ratio, following the concepts of reference 10. Since E and E' as used herein are in themselves only approximations for elliptic wings, it should be realized that the results given by the present method at zero lift will not agree exactly with the values which would be obtained by using lifting-surface solutions for a given two-dimensional lift-curve slope. However, such differences are expected to be insignificant.

The calculations for wings having no twist or continuous twist are discussed in the following section and are illustrated by means of example calculations for an untwisted wing designated as wing A. The calculations for wings with discontinuous twist require a slightly different procedure and therefore are discussed in an additional section. The latter calculations are illustrated by means of example calculations for a wing with partial-span flaps designated as wing B.

WINGS WITH NO TWIST OR CONTINUOUS TWIST

The rolling motion of a wing produces an antisymmetric linear aerodynamic twist distribution which gives rise to the rolling derivatives. In the method of calculation used herein, the aerodynamic twist produced by the rolling motion is treated as a wing twist for purposes of obtaining the distribution of α_i. Components of the inclined force vectors are then found, from which the rolling derivatives are determined.

Use of section data.—The two-dimensional data at the Reynolds number appropriate to each wing station are simply plotted against an effective angle, $\alpha_e=\alpha_0 E$. Either the section lift coefficients c_l or the load coefficients $c_l c/b$ can be used, although the use of the latter is believed to result in considerable savings in computing time. The load coefficients were used in the example calculations for wing A and are presented in figure 1. A single drag curve was used inasmuch as no account was taken of the spanwise variation in Reynolds number due to taper; the curve is presented in figure 2. The curves in figures 1 and 2 are based on data taken from reference 11 for the NACA 65–006 section at a Reynolds number of 3.0×10^6; however, the drag data were

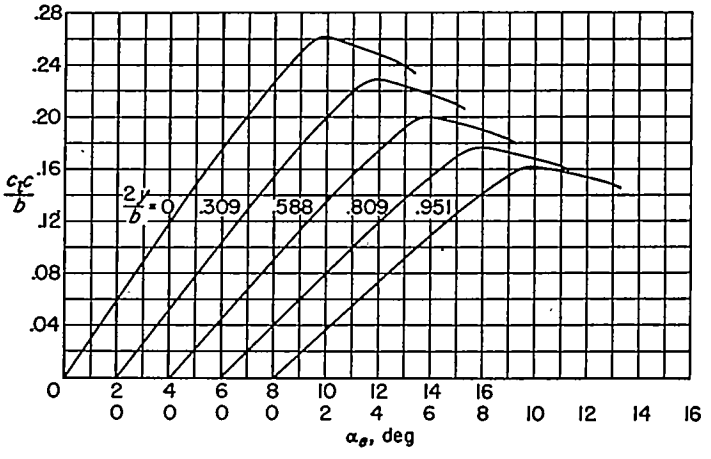

FIGURE 1.—Section loading curves used in the example calculations for wing A.

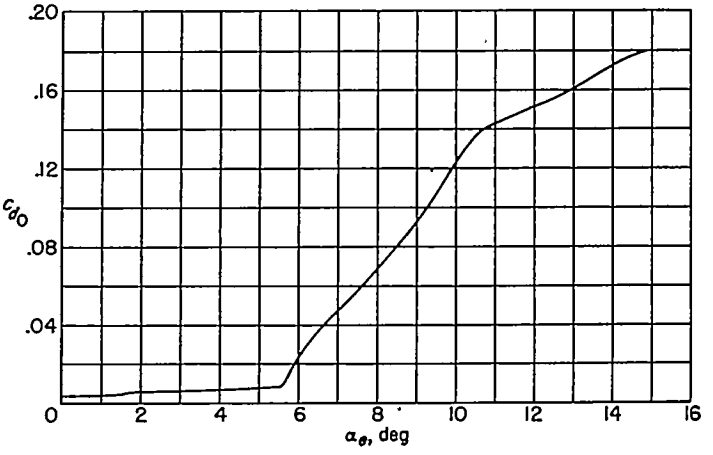

FIGURE 2.—Section drag curve used in the example calculations for wing A.

extrapolated to higher angles of attack on the basis of results in reference 12 for the NACA 64A006 section.

Determination of the lift distribution.—The effective angle of attack at any station y is given by

$$\alpha_e=\alpha-\alpha_i-\Delta\alpha_e \tag{1}$$

$$\alpha_e=\alpha_s+\epsilon+\epsilon_p-\alpha_i-\Delta\alpha_e \tag{2}$$

where

$$\epsilon_p=\frac{180}{\pi}\frac{py}{V} \tag{3}$$

$$\alpha_i=\sum_{m=1}^{r-1}\left(\frac{c_lc}{b}\right)_m\beta_{mk} \tag{4}$$

and

$$\Delta\alpha_e=\frac{E'-E}{2E'}\left[(\alpha-\alpha_i)_k-(\alpha-\alpha_i)_{r-k}\right] \tag{5}$$

The evaluation of equation (1) by the method of reference 7 is one of successive approximations, in which a distribution of c_lc/b is initially assumed. From this distribution and with the values of the multipliers β_{mk} given either in table I for $r=10$ or in reference 7 for $r=20$, a distribution of α_i is obtained by using equation (4); equation (5) can then be evaluated. With all the components on the right-hand side of equation (2) determined, it is possible to find α_e. Values of c_l corresponding to the values of α_e are found from appropriate section data, after which a check distribution of c_lc/b can be obtained. If these check values of c_lc/b do not agree with those initially assumed, new values are assumed and the process is repeated until agreement is obtained. In the following examples, methods are indicated by which the differences between the check and initially assumed values are utilized to obtain the succeeding assumed values so that agreement is reached in a minimum number of approximations. Equation (5) corrects the effective angle to account for the E' factor that is used with the antisymmetric component of loading when the section data are plotted against $\alpha_e=\alpha_0E$.

Determination of the rolling-moment and yawing-moment coefficients.—After the distributions of c_lc/b and $c_{d_0}c/b$ are determined (distributions of $c_{d_0}c/b$ are obtained by using the plots of section data), components of these distributions along the x- and z-axes in the wind-axes system give the following expressions:

$$\frac{c_xc}{b}=\frac{c_{d_0}c}{b}\cos(\epsilon_p-\alpha_i)-\frac{c_lc}{b}\sin(\epsilon_p-\alpha_i) \tag{6}$$

$$\frac{c_zc}{b}=\frac{c_lc}{b}\cos(\epsilon_p-\alpha_i)+\frac{c_{d_0}c}{b}\sin(\epsilon_p-\alpha_i) \tag{7}$$

For the angles usually encountered,

$$\cos(\epsilon_p-\alpha_i)\approx 1$$

and

$$\sin(\epsilon_p-\alpha_i)\approx\frac{\pi}{180}(\epsilon_p-\alpha_i)$$

so that equations (6) and (7) become

$$\frac{c_xc}{b}=\frac{c_{d_0}c}{b}-\frac{c_lc}{b}\frac{\pi}{180}(\epsilon_p-\alpha_i) \tag{8}$$

$$\frac{c_zc}{b}=\frac{c_lc}{b}+\frac{c_{d_0}c}{b}\frac{\pi}{180}(\epsilon_p-\alpha_i) \tag{9}$$

It is easily seen that, for $\epsilon_p=0°$, equations (8) and (9) reduce to the usual expressions for the section contributions to the lift and drag of a nonrolling wing inasmuch as the contribution of c_{d_0} to the lift in equation (9) is usually negligible.

Spanwise integrations of equations (8) and (9) yield the yawing-moment and rolling-moment coefficients as follows:

$$C_n=\frac{A}{4}\int_{-1}^{1}\left[c_{d_0}-c_l\frac{\pi}{180}(\epsilon_p-\alpha_i)\right]\frac{c}{b}\frac{2y}{b}\,d\frac{2y}{b} \tag{10}$$

$$C_n\approx A\sum_{m=1}^{r-1}\left[\left(\frac{c_{d_0}c}{b}\right)_m-\frac{\pi}{180}\left(\frac{c_lc}{b}\right)_m(\epsilon_p-\alpha_i)_m\right]\sigma_m \tag{10a}$$

$$C_l=-\frac{A}{4}\int_{-1}^{1}\left[c_l+c_{d_0}\frac{\pi}{180}(\epsilon_p-\alpha_i)\right]\frac{c}{b}\frac{2y}{b}\,d\frac{2y}{b} \tag{11}$$

$$C_l\approx -A\sum_{m=1}^{r-1}\left[\left(\frac{c_lc}{b}\right)_m+\frac{\pi}{180}\left(\frac{c_{d_0}c}{b}\right)_m(\epsilon_p-\alpha_i)_m\right]\sigma_m \tag{11a}$$

Values of the numerical integrating multipliers σ_m are given in table II for $r=10$ and $r=20$ in addition to the area multipliers η_m. The η_m multipliers may be used to find C_L and C_D by similar relations, that is, $C_L=A\sum_{m=1}^{r-1}\left(\frac{c_lc}{b}\right)_m\eta_m$, and so forth.

TABLE I.—INDUCED-ANGLE-OF-ATTACK MULTIPLIERS β_{mk} FOR ASYMMETRICAL LIFT DISTRIBUTIONS WITH $r=10$ [1]

$$\left[\alpha_{i_k}=\sum_{m=1}^{9}\left(\frac{c_lc}{b}\right)_m\beta_{mk}\right]$$

$\frac{2y}{b}$		−0.9511	−0.8090	−0.5878	−0.3090	0		
$\frac{2y}{b}$	m \ k	9	8	7	6	5		
−0.9511	9	231.766	−43.879	0	−2.148	0	1	0.9511
−.8090	8	−83.463	121.847	−34.405	0	−2.573	2	.8090
−.5878	7	0	−47.354	88.527	−29.824	0	3	.5878
−.3090	6	−6.610	0	−35.060	75.305	−28.532	4	.3090
0	5	0	−4.377	0	−30.000	71.620	5	0
.3090	4	−1.716	0	−3.388	0	−28.532	6	−.3090
.5878	3	0	−1.188	0	−2.882	0	7	−.5878
.8090	2	−.544	0	−.863	0	−2.573	8	−.8090
.9511	1	0	−.286	0	−.558	0	9	−.9511
		1	2	3	4	5	k \ m	$\frac{2y}{b}$
		0.9511	0.8090	0.5878	0.3090	0	$\frac{2y}{b}$	

[1] Values of k at top to be used with values of m at left side; values of k at bottom to be used with values of m at right side.

Application of the method.—In order to illustrate the use of the method, an example is presented for wing A at an angle of attack of 12°, rolling at such a rate that the wing-tip helix angle $pb/2V$ is 0.01 radian. The calculations are made for $r=10$. The pertinent dimensional data are given in table III and the lift distribution is calculated in table IV.

The initially assumed load distribution in the linear lift range can be most rapidly obtained by using methods with which the reader is probably already familiar. For example, nearly exact initial assumptions can be made very quickly by proper use of the numerous lifting-surface solutions which are available in chart form and thus effect appreciable savings in computing time. For the sake of presenting a numerical procedure, however, the method of reference 13, which has been shown to give very good results in most cases, was used in this report. By combining the equation of reference 7 for the initial approximation with equation (33) of reference 8 and equations (13) and (18) (modified for E') of reference 13, the following expression is obtained for the initially assumed load distribution:

$$\left(\frac{c_l c}{b}\right)_{assumed} \approx \frac{1}{2}\left[\frac{Ac}{b}+1.273\sqrt{1-\left(\frac{2y}{b}\right)^2}\right]\left[\frac{c_{l(\alpha)}}{A+1.8}+\frac{Aa_0(\epsilon-\bar{\epsilon})}{AE+6}+\frac{Aa_0\epsilon_p}{AE'+4}\right] \quad (12)$$

TABLE II.—WING-COEFFICIENT MULTIPLIERS FOR WINGS WITHOUT DISCONTINUOUS TWIST

$\frac{2y}{b}$	$r=20$			$r=10$		
	m	η_m	σ_m	m	η_m	σ_m
−0.9877	19	0.01638	−0.00809	------	----------	----------
−.9511	18	.01618	−.00769	9	0.06472	−0.03078
−.8910	17	.04754	−.02118	------	----------	----------
−.8090	16	.03078	−.01245	8	.06154	−.02489
−.7071	15	.07405	−.02618	------	----------	----------
−.5878	14	.04236	−.01245	7	.16943	−.04980
−.4540	13	.09331	−.02118	------	----------	----------
−.3090	12	.04980	−.00769	6	.09959	−.01539
−.1564	11	.10343	−.00809	------	----------	----------
0	10	.05236	0	5	.20944	0
.1564	9	.10343	.00809	------	----------	----------
.3090	8	.04980	.00769	4	.09959	.01539
.4540	7	.09331	.02118	------	----------	----------
.5878	6	.04236	.01245	3	.16943	.04980
.7071	5	.07405	.02618	------	----------	----------
.8090	4	.03078	.01245	2	.06154	.02489
.8910	3	.04754	.02118	------	----------	----------
.9511	2	.01618	.00769	1	.06472	.03078
.9877	1	.01638	.00809	-------	----------	----------

TABLE III.—GEOMETRIC CHARACTERISTICS OF WING A

Taper ratio, λ	0.60	Geometric twist, ϵ_t, deg	None
Aspect ratio, A	4.00	Edge-velocity factor, E	1.118
Root section	NACA 65-006	Edge-velocity factor, E'	1.414
Tip section	NACA 65-006	Wing Reynolds number, R	3.0×10^6

$\frac{2y}{b}$	$\frac{c}{b}$	R (assumed)	$\frac{t}{c}$	$\frac{\epsilon}{\epsilon_t}$	ϵ
0	0.3127	3.0×10^6	0.06	0	0
.309	.2740	3.0	.06	0	0
.588	.2392	3.0	.06	0	0
.809	.2115	3.0	.06	0	0
.951	.1937	3.0	.06	0	0

$$\frac{c}{b}=\frac{2}{A(1+\lambda)}\left[1-(1-\lambda)\frac{2y}{b}\right]$$

(Alter values of $\frac{c}{b}$ near tip if tip is rounded.)

TABLE IV.—CALCULATION OF LIFT DISTRIBUTION FOR WING A

$\left[\alpha_r=12.00°;\ \frac{pb}{2V}=0.01 \text{ radian}\right]$

①	②	③	④	⑤	⑥	⑦	⑧	⑨	⑩	⑪	⑫	⑬	⑭
$\frac{2y}{b}$	$\frac{cc}{b}$ (assumed)	Multipliers β_{mk}: k / 9	8	7	6	5	$\frac{cc}{b}$ reverse of ③	α_i (a)	ϵ_p	α $(\alpha_r+\epsilon+\epsilon_p)$	$\Delta\alpha_s$ (b)	$\frac{\alpha_s}{⑪-⑨-⑩}$	Check $\frac{cc}{b}$
		$\frac{2y}{b}$ / −.951	−.809	−.588	−.309	0							
−0.951	0.0901	231.766	−43.879	0	−2.148	0	0.0958	[c]6.59	−0.55	11.45	[d]−0.04	4.90	0.0901
−.809	.1494	−83.403	121.847	−34.405	0	−2.573	.1560	3.95	−.46	11.54	−.06	7.65	.1481
−.588	.1877	0	−47.354	88.527	−29.824	0	.1939	2.97	−.34	11.66	−.05	8.74	.1877
−.309	.2183	−6.610	0	−35.060	75.305	−28.532	.2220	2.93	−.18	11.82	−.03	8.92	.2183
0	.2369	0	−4.377	0	−30.000	71.620	.2369	3.62	0	12.00	0	8.38	.2369
.309	.2220	−1.716	0	−3.388	0	−28.532	.2183	[c]3.03	.18	12.18	.03	9.12	.2220
.588	.1939	0	−1.188	0	−2.883	0	.1877	3.15	.34	12.34	.05	9.14	.1939
.809	.1560	−.544	0	−.863	0	−2.573	.1484	4.34	.46	12.46	.06	8.13	.1560
.951	.0958	0	−.286	0	−.558	0	.0901	7.26	.55	12.55	.04	5.24	.0959
		$\frac{2y}{b}$ / .951	.809	.588	.309	0							
		k / 1	2	3	4	5							

[a] $\alpha_{i_k}=\Sigma③\times\beta_{mk}$ for $9\geq k\geq5$; $\alpha_{i_k}=\Sigma④\times\beta_{mk}$ for $5\geq k\geq1$.

[b] $\Delta\alpha_s=\frac{E'-E}{2E'}[(\alpha-\alpha_i)_k-(\alpha-\alpha_i)_{10-k}]$.

[c] $\alpha_i=\Sigma⑧\times⑨$.

[d] $\Delta\alpha_s=\frac{1.414-1.118}{2(1.414)}[(11.45-6.59)-(12.55-7.26)]\approx-0.04$.

[e] $\alpha_i=\Sigma⑧\times⑨$.

where $c_{l(\alpha)}$ is the section lift coefficient for the geometric angle of attack in question. This loading is entered in column ② of table IV in normal order and in column ⑧ in reverse order. The loading is entered in this manner in order to shorten the size of the computing form. The mechanics of computing are all self-explanatory and it will be noted that the correction to the antisymmetric part of the loading is made in column ⑫ as obtained by using equation (5). For the sake of brevity only the final calculations have been shown in the table. The check load coefficients in column ⑭, read from the section plots, will usually not agree with the assumed values for the first approximation. The process is repeated until agreement is obtained between the assumed and check values of $c_l c/b$. The manner used in determining the succeeding assumptions is dependent on a number of factors such as the linearity and the slopes of the section loading curves and on whether $r=10$ or $r=20$. Various methods for obtaining succeeding assumptions are presented in the appendix. When calculations are being made for more than one angle of attack, the first assumption for the second angle of attack can be based on the solution for the previous angle of attack by finding the value of $c_l c/b$ corresponding to an angle

$$\alpha_{s_2}=\alpha_{s_1}+(\alpha_{s_2}-\alpha_{s_1})\frac{d\alpha_s}{d\alpha_s} \tag{13}$$

in which it can be assumed that $\frac{d\alpha_s}{d\alpha_s}\approx 0.7$ in the linear range. Once the values of α_s have been determined for two angles of attack, plots of α_s against α_s can be made for each section. Values of $c_l c/b$ corresponding to the extrapolated values of α_s will usually give a fairly accurate first assumption and thus minimize the amount of computing required. If only limited calculations are being made, it is recommended that any calculations in the nonlinear range be based on the results of a calculation in the linear range in a manner similar to that just described. In general, this procedure will eliminate a rather arduous solution since the load distributions may change very rapidly in the nonlinear range.

After the induced angles of attack and the lift distribution are determined, then the profile-drag distribution can be determined. Inasmuch as each section is assumed to be acting two-dimensionally, the section drag coefficients are obtained at the section lift coefficients or effective angles α_s for the proper values of Reynolds and Mach numbers. The calculations are carried out in columns ② to ⑤ of table V. The calculations leading to the rolling derivatives are carried out in columns ⑥ to ⑫ and at the bottom of the table.

WINGS WITH DISCONTINUOUS TWIST

The discussion in this section is limited to the case where $r=20$; a similar method could be devised for $r=10$. It is emphasized that the method of altering the two-dimensional data, which is subsequently described, applies only up to and including maximum lift and therefore precludes the calculation of C_{l_p} and C_{n_p} beyond maximum lift.

Alteration of two-dimensional data.—The two-dimensional data to be used for wings with discontinuous twist must be altered in order to avoid a discontinuity in the spanwise distribution of maximum lift coefficient at the end of the flap or aileron since no such discontinuity exists in the

TABLE V.—CALCULATION OF THE ROLLING DERIVATIVES FOR WING A

$\left[\alpha_s=12.00°;\ \frac{pb}{2V}=0.01 \text{ radian}\right]$

① $\frac{2y}{b}$	③ α_s (table IV)	③ c_{d_0} (fig. 2)	④ $\frac{c}{b}$	⑤ $\frac{c_{d_0}c}{b}$ ③×④	⑥ ϵ_p 0.573×①	⑦ α_l (table IV)	⑧ $\epsilon_p-\alpha_l$ ⑥−⑦	⑨ $\frac{c_{d_0}c}{b}\times(\epsilon_p-\alpha_l)$ ⑤×⑧	⑩ $\frac{c_l c}{b}$ (table IV)	⑪ $\frac{c_l c}{b}\times(\epsilon_p-\alpha_l)$ ⑨×⑩	⑫ σ_m (table II)
−0.951	4.90	0.0077	0.1937	0.0015	−0.55	6.59	−7.14	−0.0106	0.0901	−0.6426	−0.03078
−.809	7.65	.0608	.2115	.0129	−.46	3.95	−4.41	−.0567	.1484	−.6544	−.02489
−.588	8.74	.0862	.2392	.0206	−.34	2.97	−3.31	−.0682	.1877	−.6207	−.04980
−.309	8.92	.0913	.2740	.0250	−.18	2.93	−3.11	−.0776	.2183	−.6778	−.01539
0	8.38	.0763	.3127	.0239	0	3.62	−3.62	−.0864	.2369	−.8578	0
.309	9.12	.0964	.2740	.0264	.18	3.03	−2.85	−.0754	.2220	−.6336	.01539
.588	9.14	.0970	.2392	.0232	.34	3.15	−2.81	−.0652	.1939	−.5449	.04980
.809	8.13	.0705	.2115	.0149	.46	4.34	−3.88	−.0578	.1560	−.6042	.02489
951	5.24	.0082	.1937	.0016	.55	7.26	−6.71	−.0107	.0958	−.6433	.03078

$$C_l\approx -A\sum ⑧\times\left(⑧+\frac{\pi}{180}⑥\right)=-0.00293$$

$$C_{l_p}\approx\frac{C_l}{\frac{pb}{2V}}=\frac{-0.00293}{0.01}=-0.293$$

$$C_n\approx A\sum ⑧\times\left(⑧-\frac{\pi}{180}⑩\right)=0.00042$$

$$C_{n_p}\approx\frac{C_n}{\frac{pb}{2V}}=\frac{0.00042}{0.01}=0.042$$

physical flow. The maximum lift-coefficient values are altered (see ref. 8) by the relation

$$c_{l_{max}}=(c_{l_{max}})_0+F(\Delta c_l{}^*_{max}) \tag{14}$$

where the spanwise variation of F is given for several cases in figure 3. An illustration for deriving the F factors for any wing is given in figure 4. The quantity $\Delta c_l{}^*_{max}$ is the increment in $c_{l_{max}}$ at the discontinuity due to the deflection of the flap or aileron for the proper local Reynolds number. The values of c_l and α_0 are then altered according to the equations

$$c_l=c_{l_0}\frac{c_{l_{max}}}{(c_{l_{max}})_0} \tag{15}$$

$$\alpha_s=\alpha_{l_0}+E(\alpha_0-\alpha_{l_0})\frac{c_{l_{max}}}{(c_{l_{max}})_0} \tag{16}$$

The data altered in this manner are shown plotted in figure 5 for wing B with 60-percent-span split flaps deflected 60°. For purposes of comparison the unaltered two-dimensional section data cross-plotted from reference 11 are also shown in figure 5.

The two-dimensional drag values as such are not altered, but the values of $(c_{d_0})_0$ corresponding to the values of c_{l_0} are replotted against either c_l or α_s. The drag data used in the example for wing B are shown in figure 6 plotted against

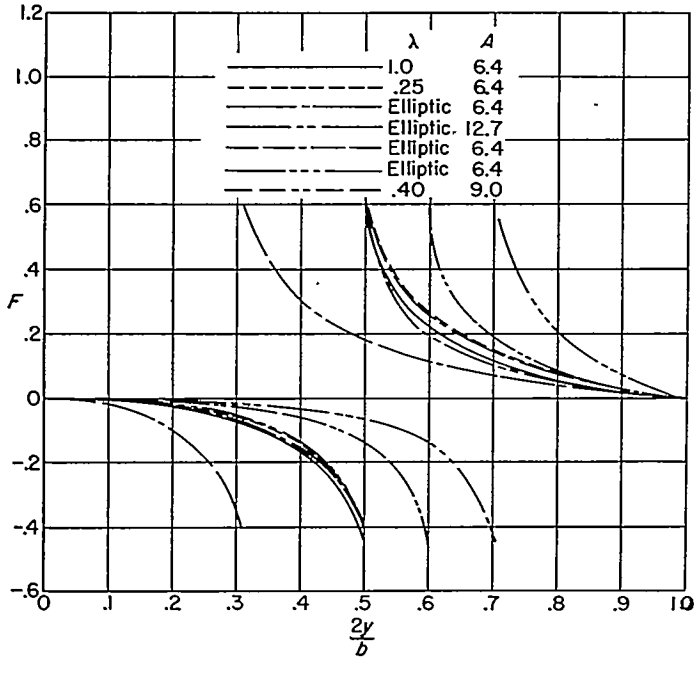

FIGURE 3.—Factor for altering two-dimensional data for several wings having discontinuous twist.

c_l. The data for the unflapped sections were taken from reference 11, cross-plotted to the values of R shown in figure 5. Since no drag data were available for the NACA 64–210 section with split flaps deflected, the data for the NACA 23012 airfoil section (ref. 14) were used inasmuch as the lift curves were similar to those for the NACA 64–210 section up to maximum lift. Since the data of reference 14 were for $R=3.5\times10^6$, no account was taken of the Reynolds number variation across the flapped portion of the span. The manner of alteration just described is necessarily arbitrary and further experimental work may indicate a different procedure; however, it should be recognized that the drag contributions depend on the differences in α_s between the right and left wings and therefore are not critically dependent on the absolute values of the drag polars.

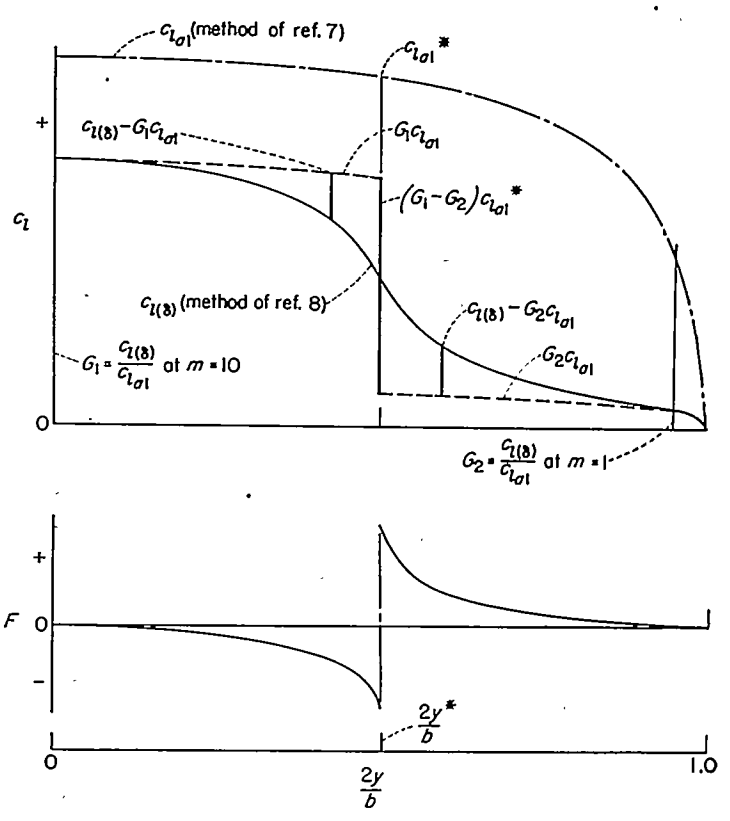

F	
Inboard	Outboard
$\frac{c_{l(\delta)}-G_1c_{l_{a1}}}{(G_1-G_2)c_{l_{a1}}{}^*}$	$\frac{c_{l(\delta)}-G_2c_{l_{a1}}}{(G_1-G_2)c_{l_{a1}}{}^*}$

FIGURE 4.—Schematic illustration of the calculation of the factor F used in altering the two-dimensional data for a wing having discontinuous twist with the discontinuities located at $\pm 2y^*/b$.

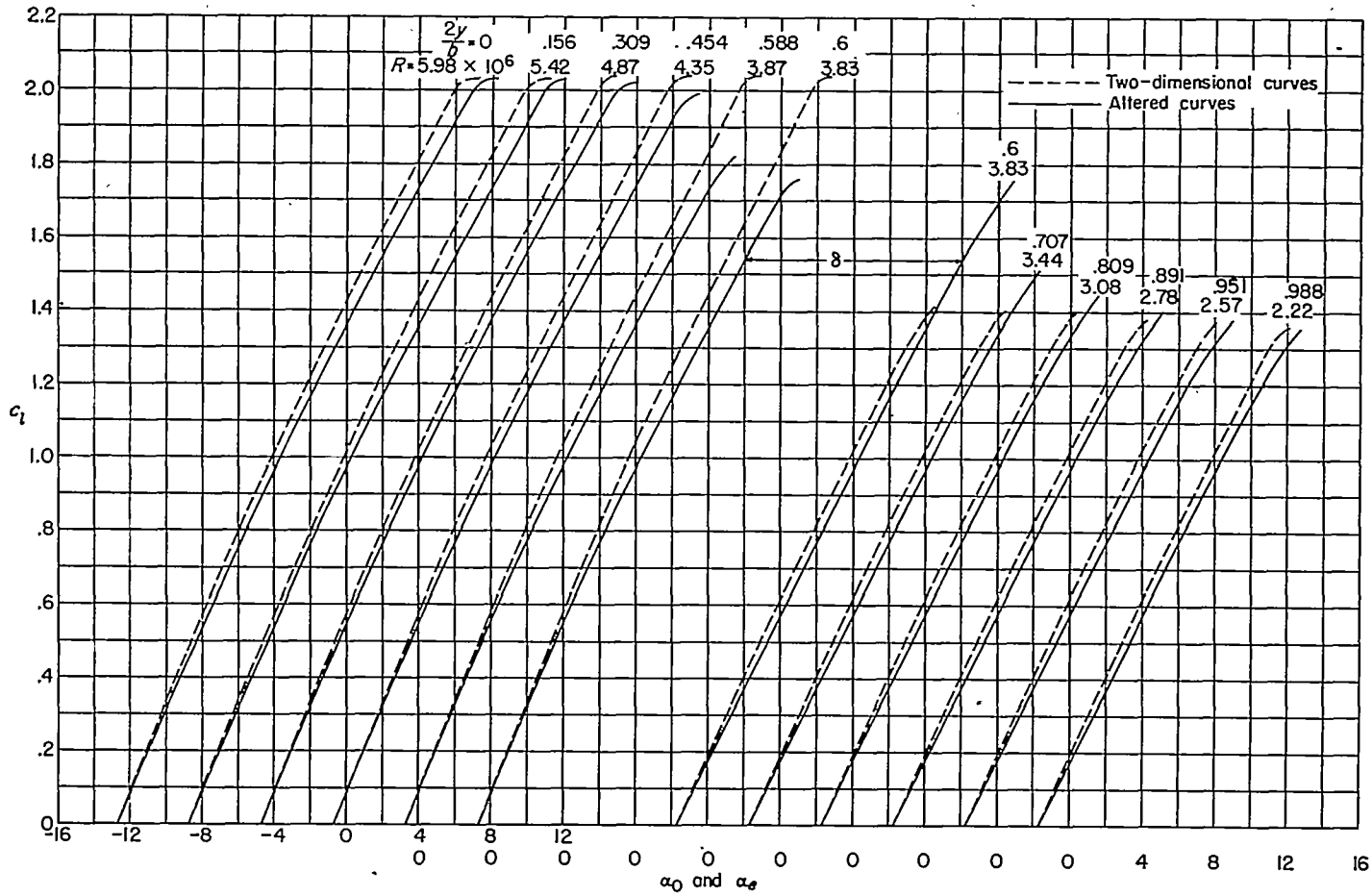

FIGURE 5.—Unaltered two-dimensional and altered section lift curves used in the example calculations for wing B. Two-dimensional curves cross-plotted from data of reference 11.

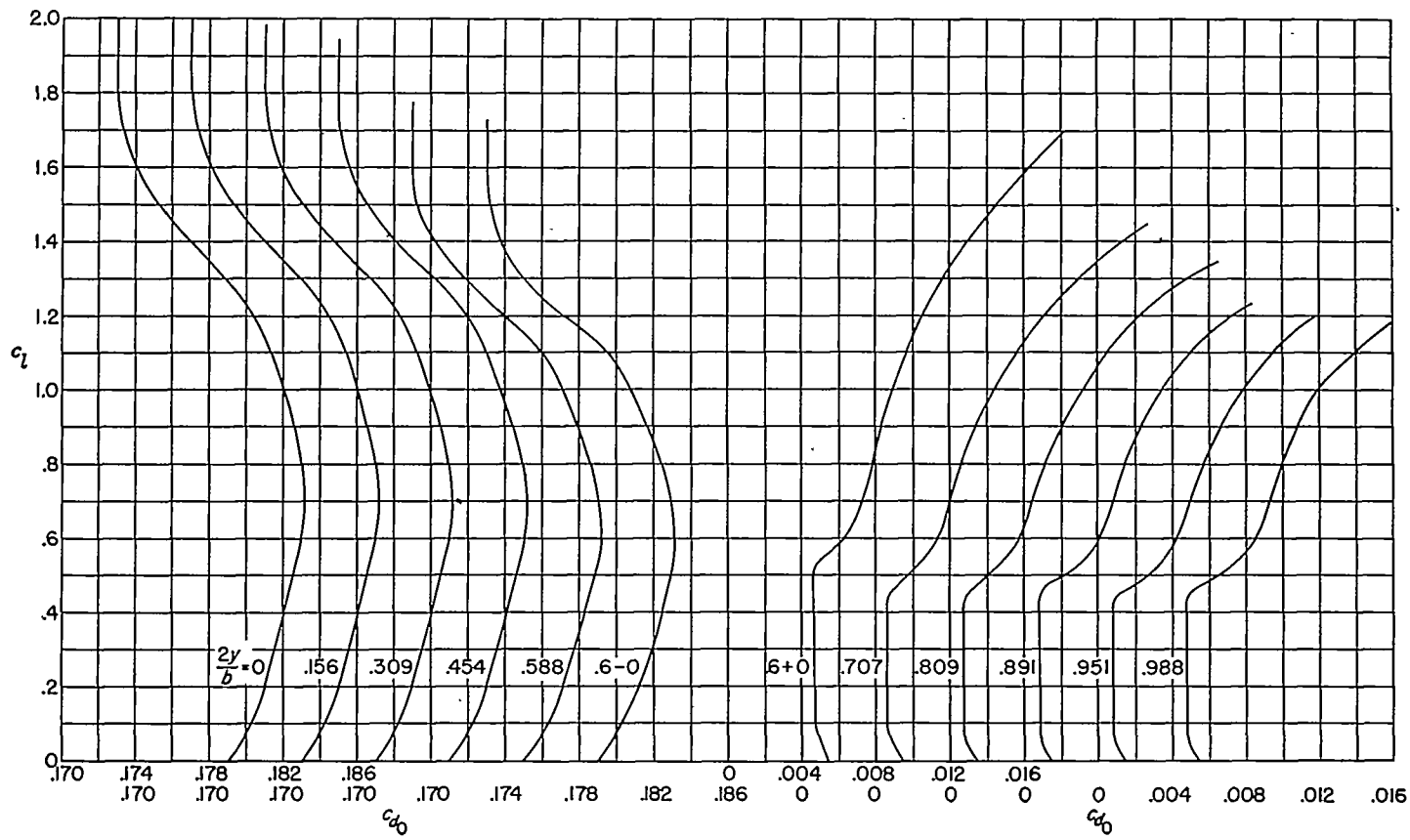

FIGURE 6.—Section drag curves used in the example calculations for wing B.

Determination of the lift distribution.—For wings with discontinuous twist the induced angle of attack computed by means of equation (4) is modified by a term which is proportional to the magnitude of the discontinuity and acts as a correction factor to account for the inability of a limited trigonometric series to represent adequately the lift distribution of a wing with partial-span flaps or ailerons deflected. This induced angle, according to reference 8, is

$$\alpha_{i_k}=\alpha_{u_k}+\delta\left(\frac{\alpha_{c_k}}{\delta}\right) \tag{17}$$

where α_{u_k} is the uncorrected induced angle of attack given by equation (4), δ is the magnitude of the discontinuity, and values of the correction factors α_{c_k}/δ taken from reference 8 are given in table VI. These correction factors depend only on the spanwise position of the discontinuity and apply to a deflected flap or aileron extending from the point of discontinuity to the right wing tip. Values for any spanwise extent of the deflection of the flap or aileron, or both, can be obtained by combinations of the values presented. For example, if the flap deflection is symmetrical and extends over 60 percent of the wing span, the values of α_c/δ would be obtained by subtracting the values of α_c/δ corresponding to $\frac{2y^*}{b}=0.6$ from those which correspond to $\frac{2y^*}{b}=-0.6$. The tabular values of α_c/δ for $\frac{2y^*}{b}=\frac{2y}{b}$ are for the flap side of the discontinuity $\left(\frac{2y^*}{b}+0\right)$; therefore the corresponding section lift curves should be used with these values. The value of δ is obtained as shown in figure 5.

If the discontinuity is located at a station other than $\frac{2y}{b}=\cos\frac{k\pi}{r}$, the values of $(c_lc/b)^*$ are interpolated from the calculated values of c_lc/b as follows:

$$\left(\frac{c_lc}{b}\right)^*=\sum_m\left(\frac{c_lc}{b}\right)_m\nu_m \tag{18}$$

values of the interpolation multipliers ν_m are given in table VII for various spanwise positions of the end of the flap. Multipliers for positions of $2y^*/b$ other than those tabulated can be calculated from the relations given in reference 8.

Application of the method.—The method is applied to wing B with 60-percent-span split flaps deflected 60° at $\alpha_s=10°$ and rolling at such a rate that the wing-tip helix angle $pb/2V$ is 0.01 radian. The geometric characteristics

TABLE VI.—ANGLE CORRECTION $\frac{\alpha_c}{\delta}$ AT STATION $\frac{2y}{b}$ DUE TO DISCONTINUITY IN INDUCED ANGLE OF ATTACK AT STATION $\frac{2y^*}{b}$

$\frac{2y^*}{b}$ \ $\frac{2y}{b}$	−0.9877	−0.9511	−0.8910	−0.8090	−0.7071	−0.5878	−0.4540	−0.3090	−0.1564	0	0.1564	0.3090	0.4540	0.5878	0.7071	0.8090	0.8910	0.9511	0.9877
−0.9877	0.4340	−0.0262	0.0029	−0.0013	0.0004	−0.0003	0.0001	−0.0001	0	0	0	0	0	0	0	0	0	0	0
−.9511	.0768	.4666	−.0324	.0039	−.0018	.0006	−.0004	.0002	−.0002	.0001	−.0001	0	0	0	0	0	0	0	0
−.9000	−.0213	.1114	.2648	−.0036	.0022	.0006	.0002	.0003	.0001	.0001	0	.0001	0	.0001	0	0	0	0	0
−.8910	−.0134	.0612	.4785	−.0358	.0044	−.0021	.0007	−.0005	.0002	−.0002	.0001	−.0001	.0001	−.0001	0	0	0	0	0
−.8090	.0078	−.0102	.0551	.4849	−.0379	.0048	−.0023	.0008	−.0006	.0002	−.0002	.0001	−.0001	.0001	−.0001	.0001	−.0001	0	−.0001
−.8000	−.0035	−.0053	.0072	−.3362	−.0657	.0068	−.0051	.0012	−.0014	.0004	−.0006	.0002	−.0003	.0001	−.0002	.0001	−.0002	.0001	−.0002
−.7071	−.0028	.0058	−.0087	.0517	.4890	−.0395	.0051	−.0025	.0008	−.0006	.0003	−.0003	.0001	−.0001	.0001	−.0001	.0001	−.0001	.0001
−.7000	−.0015	−.0011	−.0060	.0164	−.3802	−.0639	.0066	−.0051	.0012	−.0014	.0004	−.0007	.0002	−.0004	.0001	−.0003	.0001	−.0002	.0001
−.6000	.0063	−.0036	.0120	−.0117	.0876	.3154	−.0071	.0030	.0009	.0003	.0006	.0001	.0003	0	.0002	0	.0002	0	.0002
−.5878	.0021	−.0021	.0049	−.0079	.0496	.4920	−.4408	.0054	−.0027	.0009	−.0007	.0003	−.0003	.0002	−.0002	.0001	−.0001	.0001	−.0001
−.5000	−.0038	.0061	−.0059	.0124	−.0183	.0630	.0954	.0133	−.0025	.0035	−.0012	.0015	−.0006	.0009	−.0004	.0006	−.0003	.0005	−.0003
−.4540	−.0010	.0016	−.0017	.0043	−.0074	.0480	.4944	−.0419	.0057	−.0029	.0010	−.0008	.0004	−.0003	.0002	−.0002	.0001	−.0002	.0001
−.4000	.0023	−.0039	.0031	−.0064	.0056	−.0190	−.0665	−.0413	.0146	−.0075	.0034	−.0026	.0015	−.0014	.0009	−.0009	.0007	−.0008	.0006
−.3090	.0008	−.0007	.0013	−.0015	.0039	−.0070	.0467	.4964	−.0428	.0059	−.0031	.0011	−.0008	.0004	−.0004	.0002	−.0002	.0002	−.0002
−.3000	−.0007	−.0003	−.0008	−.0008	−.0006	−.0049	.0162	−.3785	−.0690	.0076	−.0063	.0015	−.0021	.0006	−.0011	.0004	−.0007	.0003	−.0006
−.2000	−.0017	.0029	−.0022	.0045	−.0042	.0107	−.0153	.0713	.1339	−.0128	−.0018	.0041	−.0012	.0020	−.0007	.0013	−.0005	.0010	−.0005
−.1564	−.0004	.0006	−.0006	.0011	−.0013	.0036	−.0067	.0457	.4983	−.0438	.0061	−.0032	.0011	−.0009	.0004	−.0004	.0003	−.0003	.0002
−.1000	.0012	−.0020	.0015	−.0027	.0022	−.0052	.0043	−.0170	−.0775	−.0491	.0157	−.0088	.0040	−.0034	.0019	.0020	.0013	−.0016	.0010
0	.0004	−.0003	.0005	−.0005	.0010	−.0012	.0034	−.0064	.0447	.5000	−.0447	.0064	−.0034	.0012	−.0010	.0005	−.0005	.0003	−.0004
.1000	−.0010	.0015	−.0013	−.0020	−.0019	.0034	−.0040	.0088	−.0157	.0491	.0775	.0170	−.0043	.0062	−.0022	.0027	−.0015	.0020	−.0012
.1564	−.0002	.0003	−.0003	.0004	−.0004	.0009	−.0011	.0032	−.0061	.0438	.5017	−.0457	.0067	−.0036	.0013	−.0011	.0006	−.0006	.0004
.2000	.0005	−.0010	.0005	−.0013	.0007	−.0020	.0012	−.0041	.0018	−.0128	−.1339	−.0713	.0153	−.0107	.0042	−.0045	.0023	−.0029	.0017
.3000	.0006	−.0003	.0007	−.0004	.0011	−.0006	.0021	−.0015	.0063	−.0076	.0690	.3785	−.0162	.0049	−.0006	.0008	.0008	.0003	.0007
.3090	.0002	−.0002	.0002	−.0002	.0004	−.0004	.0008	−.0011	.0031	−.0059	.0428	.5036	−.0467	.0070	−.0039	.0015	−.0013	.0007	−.0008
.4000	−.0006	.0008	−.0007	.0009	−.0009	.0014	−.0015	.0026	−.0034	.0075	−.0146	.0413	.0665	.0190	−.0056	.0064	−.0031	.0039	−.0023
.4540	−.0001	.0002	−.0001	.0002	−.0002	.0003	−.0004	.0008	−.0010	.0029	−.0057	.0419	.5056	−.0480	.0074	−.0043	.0017	−.0010	.0010
.5000	.0003	−.0005	.0003	−.0006	.0004	−.0009	.0006	−.0015	.0012	−.0035	.0025	−.0133	−.0954	−.0630	.0183	−.0124	.0059	−.0061	.0038
.5878	.0001	−.0001	.0001	−.0001	.0002	−.0002	.0003	−.0003	.0007	−.0009	.0027	−.0054	.0408	.5080	−.0496	.0079	−.0049	.0021	−.0021
.6000	−.0002	0	−.0002	0	−.0002	0	−.0003	−.0001	−.0006	−.0003	−.0009	−.0030	.0071	−.3154	−.0876	.0117	−.0120	.0030	−.0063
.7000	−.0001	.0002	−.0001	.0003	−.0001	.0004	−.0002	.0007	−.0004	.0014	−.0012	.0051	−.0066	.0639	.3802	−.0164	.0060	.0011	.0015
.7071	−.0001	.0001	−.0001	.0001	−.0001	.0001	−.0001	.0003	−.0003	.0006	−.0008	.0025	−.0051	.0395	.5110	−.0517	.0087	−.0058	.0028
.8000	.0002	−.0001	.0002	−.0001	.0002	−.0001	.0003	−.0002	.0006	−.0004	.0014	−.0012	.0051	−.0068	.0657	.3362	−.0072	.0053	.0035
.8090	.0001	0	.0001	−.0001	.0001	−.0001	.0001	−.0001	.0002	−.0002	.0006	−.0008	.0023	−.0048	.0379	.5151	−.0551	.0102	−.0078
.8910	0	0	0	0	0	.0001	−.0001	.0001	−.0001	.0002	−.0002	.0005	−.0007	.0021	−.0044	.0358	.5215	−.0612	.0134
.9000	0	0	0	0	0	−.0001	0	−.0001	0	−.0001	−.0001	−.0003	−.0002	−.0006	−.0022	.0036	−.2648	−.1114	.0213
.9511	0	0	0	0	0	0	0	0	.0001	−.0001	.0002	−.0002	.0004	−.0006	.0018	−.0039	.0324	.5334	−.0768
.9877	0	0	0	0	0	0	0	0	0	0	0	.0001	−.0001	.0003	−.0004	.0013	−.0029	.0263	.5660

of the wing are given in table VIII and the calculation of the spanwise lift distribution is given in table IX. The determination of the initial assumption for the lift distribution is not given herein inasmuch as the procedure is fully illustrated for this wing in reference 8 for the symmetrical case. For the asymmetrical case the approximate antisymmetric loading given by equation (18) of reference 13 (modified for E')

$$\frac{c_l c}{b} \approx \frac{1}{2}\left[\frac{Ac}{b}+1.273\sqrt{1-\left(\frac{2y}{b}\right)^2}\right]\frac{Aa_0\epsilon_p}{AE'+4}$$

should be added to the assumed symmetrical loading given by the procedure used in the example of reference 8. Any suitable method for obtaining the assumed loading may be used, however.

TABLE VII.—INTERPOLATION MULTIPLIERS ν_m FOR OBTAINING VALUES OF $\left(\frac{c_l c}{b}\right)^*$ AT THE END OF THE FLAP

$\frac{2y}{b}$ \ $\frac{2y^*}{b}$	0.2000	0.3000	0.4000	0.5000	0.6000	0.7000	0.8000	0.9000
0	−0.2970	−0.1839	0	0	0	0	0	0
.1564	1.0008	.3203	−.1940	0	0	0	0	0
.3090	.4269	.8957	.6203	−.1274	0	0	0	0
.4540	−.1307	−.0321	.6945	.7663	−.0477	−.0337	0	0
.5878	0	0	−.1208	.4786	.9112	.1234	−.0367	0
.7071	0	0	0	−.1175	.1876	.9433	.1534	0
.8090	0	0	0	0	−.0511	−.0330	.9277	−.0431
.8910	0	0	0	0	0	0	−.0444	.8901
.9511	0	0	0	0	0	0	0	.1951
.9877	0	0	0	0	0	0	0	−.0421

The values of $\frac{\alpha_c}{\delta-}$ in column ⑯ of table IX are those for $\frac{2y^*}{b}=-0.6$ from table VI; whereas the values of $\frac{\alpha_c}{\delta+}$ in column ⑰ are the negative of those for $\frac{2y^*}{b}=0.6$ and were obtained by the procedure outlined in the previous section. The values of δ at $\pm 2y^*/b$ are found from the flapped and unflapped section curves (fig. 5) at values of c_l^* corresponding to the values of $(c_l c/b)^*$. After these approximate values for δ are determined, the check span load distribution can then be calculated. The check values of $(c_l c/b)^*$ are then interpolated from equation (18). When convergence is established (i.e., column ㉕ minus column ③ is zero), the values of α_t at $\pm 2y^*/b$ can be found. (The method given for case I of the appendix was used to obtain convergence between the assumed and check values of $c_l c/b$, columns ③ and ㉕, respectively.)

The drag distribution is calculated in columns ② to ⑤ of table X. Note that two values are given at $\frac{2y}{b}=\pm 0.60$. The values at $\frac{2y}{b}=\mp 0.60 \mp 0$ correspond to the flapped sides.

The rolling-moment and yawing-moment components are calculated in columns ⑥ to ⑫ and the coefficients and derivatives are calculated at the bottom of table X. The multipliers σ_m used in table X are tabulated in table XI. If the values of C_L and C_D are desired, the numerical integrating area multipliers of reference 8 may be used.

TABLE VIII.—GEOMETRIC CHARACTERISTICS OF WING B

Taper ratio, λ	0.400	Root section	NACA 64-210
Aspect ratio, A	9.021	Tip section	NACA 64-210
Span, b, ft	15.000	Geometric twist, ϵ_t, deg	−2.00
Root chord, c_r, ft	2.381	Edge-velocity factor, E	1.024
Wing Reynolds number, R	4.44×10^6	Edge-velocity factor, E'	1.094

$\frac{2y}{b}$	$\frac{c}{c_r}$	$\frac{c}{b}$	R	$\frac{t}{c}$	$\frac{\epsilon}{\epsilon_t}$	ϵ	ν_m	$\frac{\alpha_t}{\delta}$	F	$(c_{l_{max}})_0$	$\frac{c_{l_{max}}}{(c_{l_{max}})_0}$
0	1.0000	0.1587	5.98×10^6	0.10	0	0	0	0.0006	0	2.027	1.0000
.1564	.9062	.1438	5.42	.10	.0690	−.14	0	.0015	−.0061	2.032	.9981
.3090	.8146	.1293	4.87	.10	.1517	−.30	0	.0031	−.0293	2.037	.9910
.4540	.7276	.1155	4.35	.10	.2496	−.50	−.0477	−.0068	−.0940	2.039	.9710
.5878	.6473	.1027	3.87	.10	.3632	−.73	.9112	.3154	−.3665	2.040	.8870
.7071	.5757	.0914	3.44	.10	.4913	−.98	.1876	.0878	.1779	1.401	1.0799
.8090	.5146	.0817	3.08	.10	.6288	−1.26	−.0511	−.0117	.0789	1.393	1.0356
.8910	.4654	.0739	2.78	.10	.7658	−1.53	0	.0122	.0304	1.383	1.0133
.9511	.4293	.0681	2.57	.10	.8962	−1.77	0	−.0036	.0085	1.376	1.0039
.9877	.3720	.0590	2.22	.10	.9698	−1.94	0	.0065	0	1.361	1.0000
$\frac{2y^*}{b}=0.6$	.6400	.1016	3.83	.10	.3750	−.75			−.4458 .5542	2.040 1.411	.8626 1.2471

For tapered wings with straight-line elements from root to construction tip:

$\frac{c}{c_r}=1-(1-\lambda)\frac{2y}{b}$ (Alter values of c/c_r near tip to allow for rounding.)

$\frac{\epsilon}{\epsilon_t}=\lambda\frac{2y/b}{c/c_r}$ (Use value of c/c_r before rounding tip.)

TABLE IX.—CALCULATION OF LIFT DISTRIBUTION FOR WING B

[0.6-span split flaps deflected 60°; α_r=10.00°; $\frac{pb}{2V}$=0.01 radian]

①	②	③	④	⑤	⑥	⑦	⑧	⑨	⑩	⑪	⑫	⑬	⑭	⑮
			Multipliers β_{mk}											
$\frac{2y}{b}$	ν_m	$\frac{c_l c}{b}$ (Assumed)	k / 19	18	17	16	15	14	13	12	11	10	$\frac{c_l c}{b}$ Reverse of ③	α_m (a)
			$\frac{2y}{b}$ / −.988	−.951	−.891	−.809	−.707	−.588	−.454	−.309	−.156	0		
$\frac{2y^*_-}{b}$ −0.6	$\left(\frac{c_l c}{b}\right)^*_- = \Sigma③ \times ③$ =0.1537									$c_l^*_- = \frac{\left(\frac{c_l c}{b}\right)^*_-}{\left(\frac{c}{b}\right)^*_-}$		δ_-=12.01		
−.988	0	0.0278	915.651	−166.985	0	−7.019	0	−1.401	0	−.486	0	−.230	0.0301	[b] 4.42
−.951	0	.0492	−329.859	463.533	−122.749	0	−7.438	0	−1.792	0	−.701	0	.0531	2.25
−.891	0	.0662	0	−180.336	315.512	−96.737	0	−7.073	0	−1.920	0	−.819	.0710	.51
−.809	−.0511	.0836	−26.374	0	−125.246	243.694	−81.067	0	−6.680	0	−1.977	0	.0888	−.15
−.707	.1876	.1053	0	−17.020	0	−97.524	202.571	−71.139	0	−6.391	0	−2.026	.1103	−2.39
−.588	.9112	.1627	−7.246	0	−12.604	0	−81.392	177.054	−64.735	0	−6.228	0	.1671	2.75
−.454	−.0477	.2109	0	−5.166	0	−10.126	0	−71.296	160.761	−60.725	0	−6.192	.2140	4.41
−.309	0	.2404	−2.958	0	−4.022	0	−8.596	0	−64.817	150.611	−58.514	0	.2431	4.23
−.156	0	.2635	0	−2.241	0	−3.322	0	−7.604	0	−60.768	145.025	−57.812	.2650	4.76
0	0	.2767	−1.468	0	−1.804	0	−2.865	0	−6.950	0	−58.533	143.239	.2767	5.88
.156	0	.2650	0	−1.153	0	−1.518	0	−2.554	0	−6.530	0	−57.812	.2035	[b] 4.81
.309	0	.2431	−.810	0	−.946	0	−1.319	0	−2.340	0	−6.288	0	.2404	4.30
.454	0	.2146	0	−.646	0	−.800	0	−1.176	0	−2.192	0	−6.192	.2109	4.52
.588	0	.1671	−.467	0	−.530	0	−.691	0	−1.068	0	−2.092	0	.1027	2.87
.707	0	.1103	0	−.368	0	−.441	0	−.604	0	−.981	0	−2.026	.1053	−2.20
.809	0	.0888	−.261	0	−.291	0	−.366	0	−.528	0	−.903	0	.0830	.12
.891	0	.0710	0	−.192	0	−.225	0	−.297	0	−.452	0	−.819	.0602	.83
.951	0	.0531	−.118	0	−.130	0	−.161	0	−.224	0	−.361	0	.0402	2.71
.988	0	.0301	0	−.060	0	−.069	0	−.090	0	−.133	0	−.230	.0278	5.07
$\frac{2y^*_+}{b}$ 0.6	$\left(\frac{c_l c}{b}\right)^*_+ = \Sigma③ \times ⑨$ =0.1682									$c_l^*_+ = \frac{\left(\frac{c_l c}{b}\right)^*_+}{\left(\frac{c}{b}\right)^*_+}$		δ_+=12.07		
			$\frac{2y}{b}$ / .988	.951	.891	.809	.707	.588	.454	.309	.156	0		
			k / 1	2	3	4	5	6	7	8	9	10		

[a] $\alpha_{m_k} = \Sigma③ \times \beta_{mk}$ for $19 \geqq k \geqq 10$; $\alpha_{m_k} = \Sigma⑩ \times \beta_{mk}$ for $10 \geqq k \geqq 1$.

[b] $\Delta\alpha_s = \frac{E'-E}{2E'}\left[(\alpha-\alpha_l)_k - (\alpha-\alpha_l)_{20-k}\right]$.

[c] $\alpha_m = \Sigma③ \times ④$.

[d] $\Delta\alpha_s = \frac{1.094-1.024}{2(1.094)}\left[(7.49-4.50)-(8.63)\,(5.15)\right] = -0.02$.

[e] $\alpha_m = \Sigma⑭ \times ⑭$.

⑯	⑰	⑱	⑲	⑳	㉑	㉒	㉓	㉔	㉕
$\frac{\alpha_s}{\delta_-}$	$\frac{\alpha_s}{\delta_+}$	$\frac{\alpha_s}{⑯\times\delta_- + ⑰\times\delta_+}$	$\frac{\alpha}{(\alpha_s+\epsilon+\epsilon_p)}$	α_l ⑯+⑱	$\Delta\alpha_s$ (b)	$\frac{\alpha_s}{⑱-⑲}$	c_l (Section data)	$\frac{c}{b}$	Check $\frac{c_l c}{b}$ ㉓×㉔
$\frac{2y_-^*}{b}-0$			8.91	−4.72	−0.02	13.65			
$\frac{2y_-^*}{b}+0$				7.29	−.02	1.64	1.513	0.1016	0.1537
0.0063	0.0002	0.08	7.49	4.50	[d]−.02	3.01	.467	.0590	.0276
−.0036	0	−.04	7.68	2.21	−.02	5.49	.723	.0681	.0492
.0120	.0002	.15	7.96	.66	−.02	7.32	.895	.0739	.0661
−.0117	0	−.14	8.28	−.29	−.02	8.59	1.025	.0817	.0837
.0876	.0002	1.05	8.61	−1.34	−.02	9.97	1.152	.0914	.1053
.3154	0	3.79	8.94	6.54	−.02	2.42	1.584	.1027	.1627
−.0071	.0003	−.08	9.24	4.33	−.01	4.90	1.826	.1155	.2109
.0030	.0001	.04	9.52	4.27	−.01	5.26	1.859	.1293	.2404
.0009	.0006	.02	9.77	4.78	0	4.99	1.833	.1438	.2636
.0003	.0003	.01	10.00	5.89	0	4.11	1.743	.1587	.2766
.0006	.0009	.02	9.95	4.83	0	5.12	1.843	.1438	.2650
.0001	.0030	.04	9.87	4.34	.01	5.52	1.880	.1293	.2431
.0003	−.0071	−.08	9.76	4.44	.01	5.31	1.858	.1155	.2146
0	.3154	3.81	9.61	6.68	.02	2.91	1.626	.1027	.1670
.0002	.0876	1.06	9.42	−1.14	.02	10.54	1.207	.0914	.1103
0	−.0117	−.14	9.21	−.02	.02	9.21	1.087	.0817	.0888
.0002	.0120	.15	8.98	.98	.02	7.98	.961	.0739	.0710
0	−.0036	−.04	8.77	2.68	.02	6.07	.778	.0681	.0530
.0002	.0063	.08	8.63	5.15	.02	3.46	.514	.0590	.0303
$\frac{2y_+^*}{b}-0$			9.59	7.43	.02	2.14	1.557	.1016	.1582
$\frac{2y_+^*}{b}+0$				−4.64	.02	14.21			

TABLE X.—CALCULATION OF THE ROLLING DERIVATIVES FOR WING B

[0.6-span split flaps deflected 60°; α_r=10.00°; $\frac{pb}{2V}$=0.01 radian]

① $\frac{2y}{b}$	② c_l (table IX)	③ c_{d_0} (fig. 6)	④ $\frac{c}{b}$	⑤ $\frac{c_{d_0}c}{b}$ ③×④	⑥ ϵ_p 0.573×①	⑦ α_l (table IX)	⑧ $\epsilon_p-\alpha_l$ ⑥−⑦	⑨ $\frac{c_{d_0}c}{b}\times(\epsilon_p-\alpha_l)$ ⑤×⑧	⑩ $\frac{c_lc}{b}$ (table IX)	⑪ $\frac{c_lc}{b}\times(\epsilon_p-\alpha_l)$ ⑧×⑩	⑫ σ_m (table XI)
−0.988	0.467	0.0054	0.0590	0.00032	−0.57	4.50	−5.07	−0.0016	0.0278	−0.1410	−0.00809
−.951	.723	.0092	.0681	.00063	−.54	2.21	−2.76	−.0017	.0492	−.1358	−.00769
−.891	.895	.0103	.0739	.00076	−.51	.66	−1.17	−.0009	.0662	−.0774	−.02118
−.809	1.025	.0115	.0817	.00094	−.46	−.29	−.17	−.0002	.0836	−.0142	−.01272
−.707	1.152	.0123	.0914	.00112	−.41	−1.34	.94	.0011	.1053	−.0990	−.02498
−.600−0	1.513	.0147	.1016	.00149	−.34	−4.72	4.38	.0065	.1537	.6732	−.00534
−.600+0	1.513	.1731	.1016	.01759	−.34	7.29	−7.65	−.1342	.1537	−1.1727	−.00088
−.588	1.584	.1730	.1027	.01777	−.34	6.54	−6.88	−.1222	.1627	−1.1194	−.00716
−.454	1.826	.1730	.1155	.01998	−.26	4.33	−4.59	−.0917	.2109	−.9680	−.02118
−.309	1.859	.1730	.1293	.02237	−.18	4.27	−4.45	−.0995	.2404	−1.0093	−.00769
−.156	1.833	.1730	.1438	.02488	−.09	4.78	−4.87	−.1211	.2635	−1.2833	−.00809
0	1.743	.1731	.1587	.02747	0	5.89	−5.89	−.1618	.2767	−1.6298	0
.156	1.843	.1730	.1438	.02488	.09	4.83	−3.74	−.0930	.2650	−.9911	.00809
.309	1.880	.1730	.1293	.02237	.18	4.34	−4.16	−.0931	.2431	−1.0113	.00760
.454	1.858	.1730	.1155	.01998	.26	4.44	−4.18	−.0835	.2146	−.8970	.02118
.588	1.626	.1730	.1027	.01777	.34	6.68	−6.34	−.1126	.1671	−1.0594	.00716
.600−0	1.557	.1730	.1016	.01758	.34	7.43	−7.09	−.1246	.1582	−1.1216	.00088
.600+0	1.557	.0155	.1016	.00158	.34	−4.64	4.98	.0078	.1582	.7878	.00534
.707	1.207	.0132	.0914	.00121	.41	−1.14	1.55	.0019	.1103	.1710	.02498
.809	1.037	.0123	.0817	.00100	.46	−.02	.48	.0005	.0888	.0426	.01272
.891	.961	.0110	.0739	.00081	.51	.98	−.47	−.0004	.0710	−.0334	.02118
.951	.778	.0096	.0681	.00065	.54	2.68	−2.14	−.0014	.0531	−.1136	.00769
.988	.514	.0070	.0590	.00041	.57	5.15	−4.58	−.0019	.0301	−.1379	.00809

$$C_l \approx -A\sum ⑫\times\left[⑩+\frac{\pi}{180}⑨\right]=-0.00471$$

$$C_{l_p}\approx\frac{C_l}{\frac{pb}{2V}}=\frac{-0.00471}{0.01}=-0.471$$

$$C_n \approx A\sum ⑫\times\left[⑨-\frac{\pi}{180}⑩\right]=-0.00138$$

$$C_{n_p}\approx\frac{C_n}{\frac{pb}{2V}}=\frac{-0.00138}{0.01}=-0.138$$

DISCUSSION

Lack of either experimental wing-alone rolling data or suitable two-dimensional section data prevents the making of exact correlations of this method with experiment in the vicinity of maximum lift. It was possible, however, to compare the wing-alone calculations for wing A with experimental wing-body results, since sufficient section data existed to allow the calculations to be carried slightly beyond maximum lift. The comparisons are presented in figure 7. Agreement is considered to be good when the differences between the conditions of the calculations and tests are considered. The failure of the present method to predict the increase in C_{l_p} for $5° < \alpha < 8°$ may be inherent in the method since similar experimental trends have been observed for other wings of this plan form. The differences between the calculated and experimental variations of C_{n_p} in the same angle-of-attack range could be partly associated with the previously noted increase in C_{l_p} and partly due to body-interference effects as shown in reference 15.

Calculations which included the body-induced angle-of-attack distribution on the wing were made for wing A up to 10° angle of attack. The indications were that this component of body interference had negligible effects on the calculated variations presented in figure 7. Additional calculations for wing A using a section drag of $c_l \tan \alpha$ (no leading-edge suction) yielded a C_{n_p} variation that agreed quite closely with the experimental variation in the low angle-of-attack range; such a C_{n_p} variation would indicate the possible existence of early separation in the experimental results, a likely possibility considering the low test Reynolds number and the section thickness ratio. The differences in the high lift range, particularly with regard to the C_{n_p} variations, probably can be all ascribed to body-interference

TABLE XI.—ROLLING- AND YAWING-MOMENT-COEFFICIENT MULTIPLIERS σ_m FOR WINGS WITH DISCONTINUOUS TWIST AND $r=20$ AND HAVING DISCONTINUITIES LOCATED AT $\pm\frac{2y^*}{b}$

[Values for positive $\frac{2y}{b}$ are shown; for negative $\frac{2y}{b}$, reverse signs of all multipliers]

$\pm\frac{2y^*}{b}$ \ $\frac{2y}{b}$	0	0.1564	0.3090	0.4540	0.5878	0.7071	0.8090	0.8910	0.9511	0.9877	$\frac{2y^*}{b}-0$ [a]	$\frac{2y^*}{b}+0$ [b]
0.1000	0	0.00706	0.00814	0.02118	0.01245	0.02618	0.01245	0.02118	0.00769	0.00809	0.00083	−0.00067
.1564	0	----------	.01154	.01986	.01245	.02618	.01245	.02118	.00769	.00809	.00202	.00253
.2000	0	.00756	.00898	.02061	.01245	.02618	.01245	.02118	.00769	.00809	−.00255	.00238
.3000	0	.00785	.00420	.02118	.01245	.02618	.01245	.02118	.00769	.00809	.00340	.00033
.3090	0	.00809	----------	.02118	.01245	.02618	.01245	.02118	.00769	.00809	.00385	.00385
.4000	0	.00794	.00816	.01831	.01318	.02618	.01245	.02118	.00769	.00809	.00389	−.00208
.4540	0	.00758	.01154	----------	.01867	.02464	.01245	.02118	.00769	.00809	.00662	.00662
.5000	0	.00809	.00812	.01883	.01383	.02560	.01245	.02118	.00769	.00809	−.00378	.00491
.5878	0	.00809	.00769	.02118	----------	.02618	.01245	.02118	.00769	.00809	.00623	.00623
.6000	0	.00809	.00769	.02118	.00716	.02493	.01372	.02118	.00769	.00809	.00688	.00534
.7000	0	.00809	.00769	.02006	.01770	.06186	.01263	.02118	.00769	.00809	.00771	−.04770
.7071	0	.00809	.00769	.01986	.01807	----------	.01867	.01986	.00769	.00809	.00818	.00818
.8000	0	.00809	.00769	.02118	.01372	.02498	.00716	.02118	.00769	.00809	.00534	.00688
.8090	0	.00809	.00769	.02118	.01245	.02618	----------	.02118	.00769	.00809	.00623	.00623
.8910	0	.00809	.00769	.02118	.01245	.02454	.01868	----------	.01154	.00759	.00662	.00662
.9000	0	.00809	.00769	.02118	.01245	.02618	.01280	.02958	.01034	.00773	−.01673	.00567
.9511	0	.00809	.00769	.02118	.01245	.02618	.01245	.02118	----------	.00809	.00385	.00385
.9877	0	.00809	.00769	.02118	.01245	.02618	.01245	.01986	.01154	----------	.00253	.00304

[a] For negative $\frac{2y^*}{b}$, this becomes $-\left(\frac{2y^*}{b}-0\right)=-\frac{2y^*}{b}+0$.

[b] For negative $\frac{2y^*}{b}$, this becomes $-\left(\frac{2y^*}{b}+0\right)=-\frac{2y^*}{b}-0$.

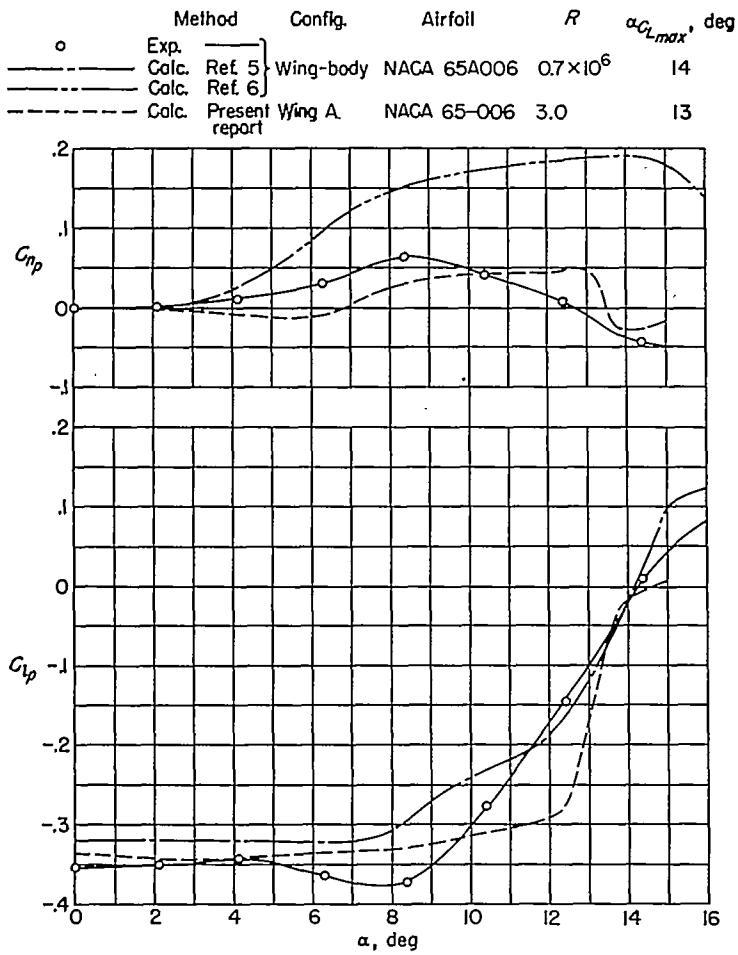

FIGURE 7.—The calculated and experimental variations of C_{l_p} and C_{n_p} with angle of attack for two wings having aspect ratios of 4.0 and taper ratios of 0.60. Experimental data from the 6-foot-diameter rolling-flow test section of the Langley stability tunnel.

effects since the differences are similar in trend to those of reference 15.

Also shown in figure 7 are the variations of C_{l_p} and C_{n_p} calculated by means of references 5 and 6, respectively, in which use is made of the experimental wing-body lift and drag curves. It appears that both the present method and that of reference 5 give reasonable estimates of the variation of C_{l_p}. The present method, however, appears to give a more realistic picture of the variation of C_{n_p} in the high angle-of-attack range than that of reference 6. The edge-suction effects which are applied in reference 6 were negligible for this aspect ratio and therefore do not account for the differences shown.

Several items of interest were observed during the course of the calculations for wing A. For example, the contributions of the section lift and profile drag to the rolling derivatives could be separated as shown in figure 8. The profile-drag component of C_{n_p} is seen to be opposite and nearly two to three times that due to the lift at high angles of attack. The profile-drag contribution to the damping in roll, on the other hand, is either zero or negligible even at the higher angles of attack.

The method presented herein is primarily intended for use in the nonlinear range where some flow separation is present, and the subsequent discussion briefly covers some considerations which limit the use of this method. The condition that must be essentially fulfilled is in keeping with the basic assumption that all sections operate two-dimensionally or nearly so. Therefore any separation that is present must not give rise to large amounts of spanwise flow which can cause a complete redistribution of lift and thus invalidate the basic assumption. Lack of sufficient experimental data on load distributions beyond maximum lift prevents the formulation of positive limits concerning these phenomena, but, on the basis of airfoil characteristics and on observed

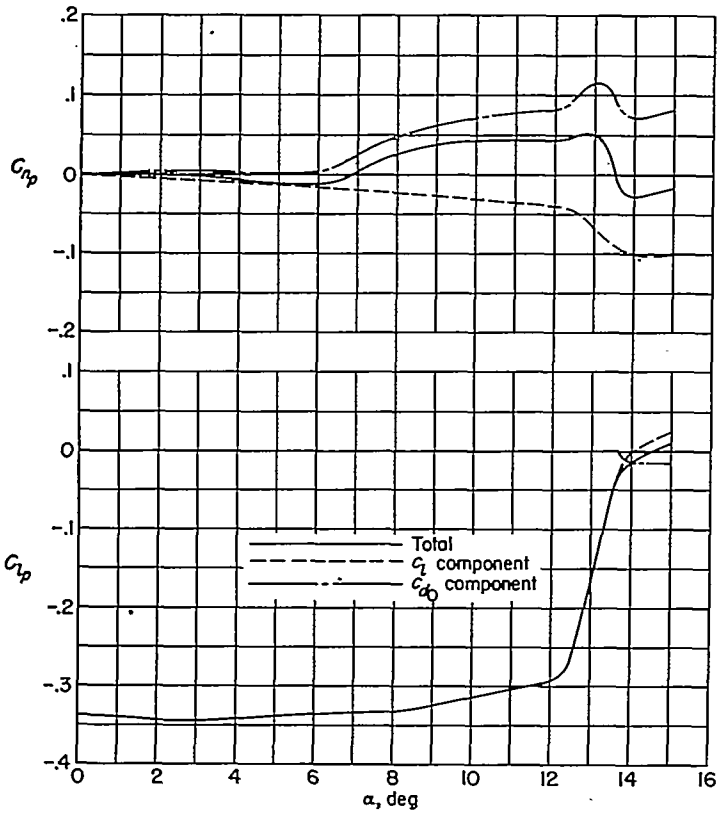

FIGURE 8.—The calculated rolling derivatives for wing A showing the lift and profile-drag components. $R=3.0\times10^6$.

stalling behavior, regions most likely to be amenable to calculation can at least be classified.

It is believed that departures from the two-dimensional-flow assumption will not seriously affect the calculation of the rolling derivatives for wings which incorporate airfoil sections that exhibit gradual changes in lift-curve slope beyond maximum lift. On the other hand, calculations beyond maximum lift for wings which incorporate sections having large discontinuities in the lift curves are believed to have little significance because with such airfoils there is no known way of predicting either the extent of the initial stall or the influence of the stalled area on the section characteristics of neighboring sections. In addition, such wings display a tendency toward asymmetrical stall under no-roll conditions which leads to rolling and yawing moments. The deflection of trailing-edge flaps generally produces abrupt lift-curve peaks at maximum lift on all but the thin airfoils. Such conditions coupled with the inability to treat the discontinuous-twist cases beyond maximum lift, as previously discussed, limit the feasibility of calculations beyond maximum lift to a very limited number of cases with full-span flaps.

Although calculations may appear to be feasible on the basis of airfoil-section stalling characteristics, there is an additional consideration which may limit the extent of the calculations. This limit, referred to in reference 16 as the stability limit, is

$$\frac{d\alpha_i}{d\alpha}<-1 \qquad (19)$$

that is, an increment in the angle of attack $\Delta\alpha$ cannot result in a decrease in the induced angle by an amount greater than the increment $\Delta\alpha$. An idea of the meaning of this limit can be obtained from the calculations for wing A. The maximum negative value in this case was -0.75 compared with -1.0 given by equation (19).

Although one has an apparent choice of performing calculations with either $r=10$ or $r=20$ for the unflapped case, it has been found from experience that calculations beyond maximum lift with $r=20$ rarely are required except perhaps at very high aspect ratios. If such calculations are necessary, however, it is suggested that the results from calculations with $r=10$ be used as the initial approximations for the $r=20$ solution, a procedure which will generally shorten computing time.

LANGLEY AERONAUTICAL LABORATORY,
NATIONAL ADVISORY COMMITTEE FOR AERONAUTICS,
LANGLEY FIELD, VA., *January 29, 1953.*

APPENDIX

METHODS FOR OBTAINING SUCCEEDING APPROXIMATIONS FOR THE SPANWISE LOAD DISTRIBUTION FROM AN INITIALLY ASSUMED LOAD DISTRIBUTION

METHODS FOR USE WITH $r=20$

These methods for obtaining succeeding approximations for the load distribution have been extensively used and produce convergence in reasonably few approximations.

Case I: $\frac{dc_l}{d\alpha}$ positive and linear.—For a positive and linear lift-curve slope, the succeeding approximation, denoted by the superscript 1, is given by the equation

$$\left(\frac{c_l c}{b}\right)_m^1 = \left(\frac{c_l c}{b}\right)_{m_{assumed}} + \Delta'\left(\frac{c_l c}{b}\right)_m \tag{A1}$$

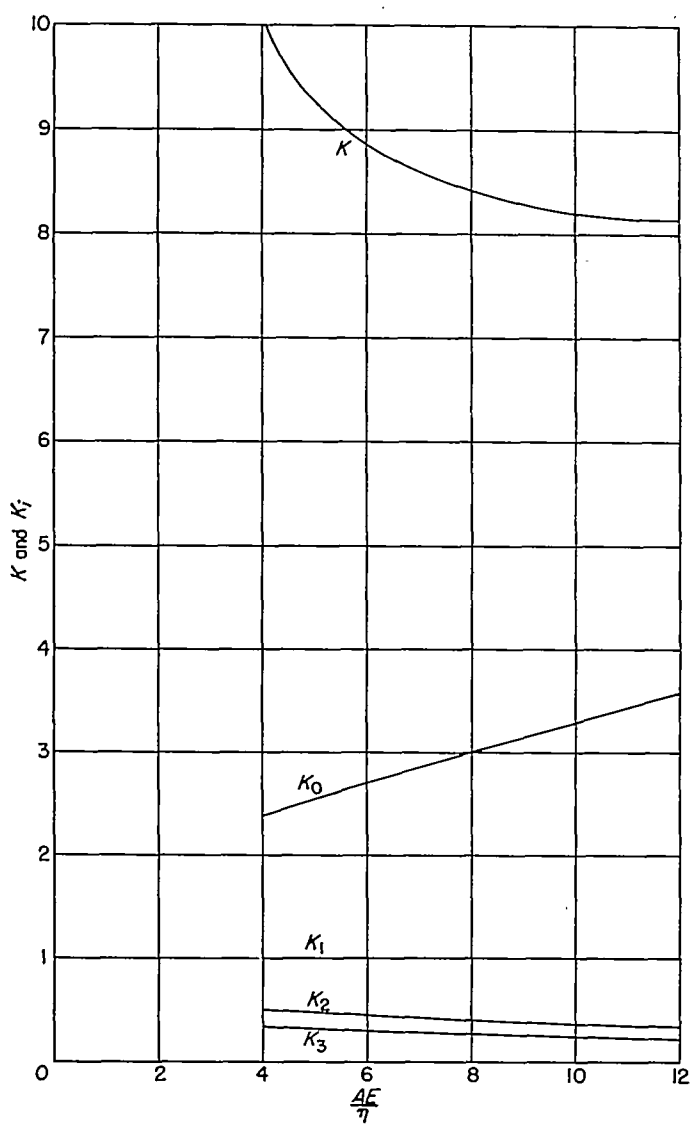

FIGURE 9.—Coefficients used to obtain succeeding approximations. $r=20$.

where

$$\Delta'\left(\frac{c_l c}{b}\right)_m = \frac{1}{K}\sum_{i=0}^{r-1} K_i \Delta\left(\frac{c_l c}{b}\right)_{m-i} \tag{A2}$$

in which the increments $\Delta\left(\frac{c_l c}{b}\right)_m$ are the differences between the check values and the assumed values (column ㉕ minus column ③, table IX), and K and K_i are constants for any particular wing. Values of K and K_i taken from reference 8 are presented in figure 9 as functions of AE/η. Values of K_i for i greater than 3 are small enough to be considered negligible.

The number of terms of equation (A2) needed for any particular approximation depends upon the convergence of the assumptions; fewer terms are needed when the differences $\Delta\left(\frac{c_l c}{b}\right)_m$ are small or when positive differences nearly cancel negative differences. Equation (A2) applied to wing B at $m=6\left(\frac{2y}{b}=0.588\right)$ becomes

$$\Delta'\left(\frac{c_l c}{b}\right)_6 = \frac{1}{8.3}\{3.2(㉕-③)_6+(㉕-③)_5+(㉕-③)_7+ 0.4[(㉕-③)_4+(㉕-③)_8]+0.3[(㉕-③)_3+(㉕-③)_9]\}$$

For $m=1$ and 2, equation (A2) is expanded as

$$\Delta'\left(\frac{c_l c}{b}\right)_1 = \frac{1}{K}\left[(K_0-K_2)\Delta\left(\frac{c_l c}{b}\right)_1+(K_1-K_3)\Delta\left(\frac{c_l c}{b}\right)_2+ K_2\Delta\left(\frac{c_l c}{b}\right)_3+K_3\Delta\left(\frac{c_l c}{b}\right)_4\right] \tag{A3}$$

$$\Delta'\left(\frac{c_l c}{b}\right)_2 = \frac{1}{K}\left[(K_1-K_3)\Delta\left(\frac{c_l c}{b}\right)_1+K_0\Delta\left(\frac{c_l c}{b}\right)_2+ K_1\Delta\left(\frac{c_l c}{b}\right)_3+K_2\Delta\left(\frac{c_l c}{b}\right)_4+K_3\Delta\left(\frac{c_l c}{b}\right)_5\right] \tag{A4}$$

since

$$\Delta\left(\frac{c_l c}{b}\right)_{-j} = -\Delta\left(\frac{c_l c}{b}\right)_j \tag{A5}$$

For $m=18$ and 19, the values of $\Delta'\left(\frac{c_l c}{b}\right)_{18}$ and $\Delta'\left(\frac{c_l c}{b}\right)_{19}$ are similar in form to the values of $\Delta'\left(\frac{c_l c}{b}\right)_2$ and $\Delta'\left(\frac{c_l c}{b}\right)_1$, respectively. For wing B, equation (A3) would be

$$\Delta'\left(\frac{c_l c}{b}\right)_1 = \frac{1}{8.3}[(3.2-0.4)(㉕-③)_1+ (1.0-0.3)(㉕-③)_2+0.4(㉕-③)_3+0.3(㉕-③)_4]$$

whereas equation (A4) would become

$$\Delta'\left(\frac{c_l c}{b}\right)_2=\frac{1}{8.3}\left[(1.0-0.3)(㉕-③)_1+3.2(㉕-③)_2+\right.$$
$$\left.1.0(㉕-③)_3+0.4(㉕-③)_4+0.3(㉕-③)_5\right]$$

Use of the K factors has been found to establish convergence within three approximations when the initial assumption is reasonably close.

Case II: $\frac{dc_l}{d\alpha}$ positive and nonlinear.—Although the factors in figure 9 were derived for a linear lift-curve slope that is constant across the span, they can be used in the nonlinear range. An estimation is made of the wing lift-curve slope at the angle of attack in question, from which a value of η is obtained. The K factors are then obtained at the proper value of AE/η. In this way it is possible to use these factors for values of η as low as 0.3 for $A=3.0$. From the trends of the variations, it is seen that considerable extrapolation is permissible at the higher values of AE/η.

Case III: $\frac{dc_l}{d\alpha}$ negative and linear or nonlinear.—For a negative lift-curve slope, either linear or nonlinear, the procedure is as follows:

(1) First obtain values of the span load distribution with fewer significant figures than desired.

(2) Find $\Delta\left(\frac{c_l c}{b}\right)$ at each station, and work with these values directly.

(3) Adjust the load distribution at those stations where the largest values of $\Delta\left(\frac{c_l c}{b}\right)$ occur by adjusting the loadings at m and $m\pm1$ stations to obtain approximate convergence at the mth station. If large values of $\Delta\left(\frac{c_l c}{b}\right)$ occur at two adjacent stations, then adjust the loading at only one of the stations, although with some practice the adjustments required at two such stations become quite obvious.

(4) As the values of $\Delta\left(\frac{c_l c}{b}\right)$ are made smaller, the number of significant figures in the solution can be increased to the desired amount.

(5) Keep all values of $\Delta\left(\frac{c_l c}{b}\right)$ either positive or negative, if possible, for easier mental manipulation.

METHODS FOR USE WITH $r=10$

Although factors similar to the K's given in case I could be derived for the corresponding condition with $r=10$, it is equally facile to use the method described under case III for all cases with $r=10$.

REFERENCES

1. Pearson, Henry A., and Jones, Robert T.: Theoretical Stability and Control Characteristics of Wings With Various Amounts of Taper and Twist. NACA Rep. 635, 1938.
2. DeYoung, John: Theoretical Antisymmetric Span Loading for Wings of Arbitrary Plan Form at Subsonic Speeds. NACA Rep. 1056, 1951. (Supersedes NACA TN 2140.)
3. Bird, John D.: Some Theoretical Low-Speed Span Loading Characteristics of Swept Wings in Roll and Sideslip. NACA Rep. 969, 1950. (Supersedes NACA TN 1839.)
4. Jones, B. Melvill: Dynamics of the Aeroplane. The Asymmetric or Lateral Moments. Vol. V of Aerodynamic Theory, div. N, ch. III, secs. 19–23 and 32–35, W. F. Durand, ed., Julius Springer (Berlin), 1935, pp. 70–73, 76–80.
5. Goodman, Alex, and Adair, Glenn H.: Estimation of the Damping in Roll of Wings Through the Normal Flight Range of Lift Coefficient. NACA TN 1924, 1949.
6. Goodman, Alex, and Fisher, Lewis R.: Investigation at Low Speeds of the Effect of Aspect Ratio and Sweep on Rolling Stability Derivatives of Untapered Wings. NACA Rep. 968, 1950. (Supersedes NACA TN 1835.)
7. Sivells, James C., and Neely, Robert H.: Method for Calculating Wing Characteristics by Lifting-Line Theory Using Nonlinear Section Lift Data. NACA Rep. 865, 1947. (Supersedes NACA TN 1269.)
8. Sivells, James C., and Westrick, Gertrude C.: Method for Calculating Lift Distributions for Unswept Wings With Flaps or Ailerons by Use of Nonlinear Section Lift Data. NACA Rep. 1090, 1952. (Supersedes NACA TN 2283.)
9. Neely, Robert H., Bollech, Thomas V., Westrick, Gertrude C., and Graham, Robert R.: Experimental and Calculated Characteristics of Several NACA 44-Series Wings With Aspect Ratios of 8, 10, and 12 and Taper Ratios of 2.5 and 3.5. NACA TN 1270, 1947.
10. Polhamus, Edward C.: A Simple Method of Estimating the Subsonic Lift and Damping in Roll of Sweptback Wings. NACA TN 1862, 1949.
11. Abbott, Ira H., Von Doenhoff, Albert E., and Stivers, Louis S., Jr.: Summary of Airfoil Data. NACA Rep. 824, 1945. (Supersedes NACA WR L-560.)
12. McCullough, George B., and Gault, Donald E.: Boundary-Layer and Stalling Characteristics of the NACA 64A006 Airfoil Section. NACA TN 1923, 1949.
13. Sivells, James C.: An Improved Approximate Method for Calculating Lift Distributions Due to Twist. NACA TN 2282, 1951.
14. Wenzinger, Carl J., and Harris, Thomas A.: Wind-Tunnel Investigation of N.A.C.A. 23012, 23021, and 23030 Airfoils With Various Sizes of Split Flap. NACA Rep. 668, 1939.
15. Letko, William, and Riley, Donald R.: Effect of an Unswept Wing on the Contribution of Unswept-Tail Configurations to the Low-Speed Static- and Rolling-Stability Derivatives of a Midwing Airplane Model. NACA TN 2175, 1950.
16. Multhopp, H.: Die Berechnung der Auftriebsverteilung von Tragflügeln. Luftfahrtforschung, Bd. 15, Lfg. 4, Apr. 6, 1938, pp. 153–169. (Available as R.T.P. Translation No. 2302, British M.A.P.)